Research Article

Journal of Environmental Nanotechnology

The Electrical Conductivity of WO_3 Nanoparticles Synthesized with PVP by the Post-Precipitation Wet Chemical Technique

R. Priya[1*], M. Sethu Raman[2], N. Senthil kumar[2], J. Chandrasekaran[2], R. Balan[3]

[1]Department of Physics, Info Institute of Engineering, Coimbatore, TN, India
[2]Department of Physics, Sri Ramakrishna Mission Vidyalaya College of Arts & Science, Coimbatore, TN, India
[3]Department of Physics, Chikkanna Government Arts College, Tiruppur, TN, India
Received: 12.07.2016 Accepted: 20.09.2016
*priyakce08@gmail.com

ABSTRACT

The low cost wet chemical technique is used to synthesis WO_3 with using polyvinyl pyrrolidone (PVP). PVP is used as stabilizing and reducing agent. The effect of stabilizer concentration varies from in the range 0.025, 0.05 and 0.1M. The structural, AC and DC electrical properties of WO3 were successfully investigated. X-ray diffraction (XRD) studies show monoclinic phase structure of prepared WO3 nanoparticles. The DC conductivity was carried out in the temperature range from 303-403K which indicate semiconductor nature. The minimum activation energy was obtained in the higher temperature region. The frequency dependence of dielectric constant (ε'), dielectric loss (tan δ) and AC conductivity of WO3 nanoparticles of different PVP concentration were measured at room temperature. The AC conductivity was found to increases with PVP concentration. The DC conductivity was carried out in the temperature range from 303-403K which indicate semiconductor nature.

Keywords: Electrical properties; WO_3; XRD.

1. INTRODUCTION

In recent years, the semiconductor transition metal oxides (TiO_2, SnO_2, WO_3, CdS and ZnO) have been widely used in electrical and optoelectronic properties because of their unique physical properties and non-toxicity (Pechini Maggio P. Barium, 1966). Tungsten oxide (WO_3) has been prepared by various techniques including hydrothermal method (Huirache-Acuña *et al.* 2009), sputtering (Yoji Yamada *et al.* 2007), spray-pyrolysis (Michael Cocivera *et al.* 2001), microwave synthesis (Markus Niederberger *et al.* 2014), pulsed laser deposition (Joni Huotari *et al.* 2015), sol-gel process (Diah Susanti *et al.* 2014) and wet chemical method (M. Arab *et al.* 2016). As known, wet chemical method allows synthesizing the nano-sized WO_3 having high controlled morphology, crystallinty purity, simplicity, and low cost. The tungsten oxide has two different valence states, namely W^{5+} and W^{6+}. The electrons transition takes place between these two valence states appears to be responsible for the conduction (Shaltout *et al.* 1996). Therefore the concentration and nature of the tungsten oxide ions determine the conductivity behavior. In this paper, we have investigated the structural and temperature-dependent DC electrical conductivity. In addition, AC electrical conductivity at room temperature has been in the frequency range of 42 Hz -5 MHz. These results may provide the valuable information about design and manufacture WO_3 based electronic devices.

2. EXPERIMENT

WO_3 nanoparticles with different PVP concentration of 0.025, 0.05 and 0.1 g were prepared by wet chemical precipitation method. Sodium tungstate dihydrate ($Na_2WO_4.2H_2O$, Merck, 99.5%), cetyltrimethyl ammonium bromide, $(C_{16}H_{33})N(CH_3)_3Br$ (Merck, 99.5%), polyvinyl pyrrolidone $(C_6H_9NO)_n$, hydrochloric acid (Merck, 99.5%) and oxalic acid dihydrate $C_2H_2O_4.2H_2O$ (Merck, >98%). Sodium tungstate dihydrate was used as a starting salt. The required amount of sodium tungstate dihydrate dissolved in deionized water is act as starting solution. Separate aqueous solution of CTAB (0.1g), PVP (0.025 g) and oxalic acid (0.1g) were prepared by dissolving in deionized water and drop wise one by one added to the starting. The solution was dropped into HCl. The pH value of all the samples was kept constant during the synthesis, leading to formation of precipitates. The occurrence of yellow colour precipitation was stirring at 80°C for 30 min. Further, the post-precipitate stage was allowed for continuously stirring solution at room temperature for 24 hours. The as-obtained precipitation was washed several times and filtered with deionized and acetone. Then, the obtained precipitation was kept in

oven at temperature of 60°C for 6 hours for drying. Finally, the dried powder was calcined at 400°C for 1 hour. The same procedure was followed for 0.05 and 0.1 g of PVP to synthesis WO_3 nanoparticles. In which, WO_3 with different PVP content can be referred as WP1 (0.025 g), WP2 (0.05 g) and WP3 (0.1 g).

The structural properties of synthesized powders were carried out using Bruker AXS D8 Advance X-ray diffraction meter (XRD). DC electrical conductivity studies were made by using a Keithley 6517B electrometer at different temperatures. Dielectric measurements are carried out using a HIOKI 3532-50 LCR Hi-TESTER as a function of frequency from 42 Hz to 5 MHz at room temperature.

3. RESULTS & DISCUSSION

The $_{crystalline}$ and phase purity of the calcined WO_3 nanoparticles have been understand through X-ray analysis. Several diffraction peaks 23.09°, 23.65°, 24.14° , 28.29°, 29.06° and 42.98° are seen in the X-ray pattern which is well matched to the monoclinic WO_3 structures as shown in Fig. 1. The well defined diffraction peaks agrees well with the reported value in JCPDS card No.72-1465 (Powder Diffraction File). The intensity of diffraction peak (200) higher than that of the other peaks indicated that the preferential particles growth along the a-axis. The crystalline nature of WO_3 nanoparticles appears due to the sharp diffraction peaks. The crystlite size (D) of the WO_3 nanoparticles was calculated by the following relation:

$$D = \frac{k\lambda}{\beta \cos\theta} \text{------(1)}$$

where λ is the X-ray wavelength (1.54 Å), β is the FWHM in radians, and θ is the diffraction angle. The calculated crystallite sizes of the WP1, WP2 and WP3 are 40.18, 28.53 and 15.57 nm, respectively. These results show that crystallite size decreases with increasing PVP content. At the same time, the intensity of diffraction peaks increases with increasing PVP content.

The dielectric constant (ε'), dielectric loss (tan δ) and AC conductivity (σ_{ac}) were calculated in the frequency range from 42 Hz to 5 MHz for WO_3 nanoparticles at room temperature. Fig. 2 and Fig. 3 show dielectric constant and dielectric loss of WO_3 with different content of PVP. The value of dielectric constant initially decreased with increasing frequency and reaches a constant at high frequency. The observed result explains all the samples exhibits the constant dielectric value in the higher frequency region. The high value of dielectric constant at lower frequency can be explained on the basis of interfacial/space charge polarization due to grain boundary defects (Ansari *et al*. 2012). Therefore, the hopping of electrons between energy states cannot be followed the applied alternative field at the higher frequency regime. The reduction in the dielectric constant with increase in PVP content can be improved electrical conductivity.

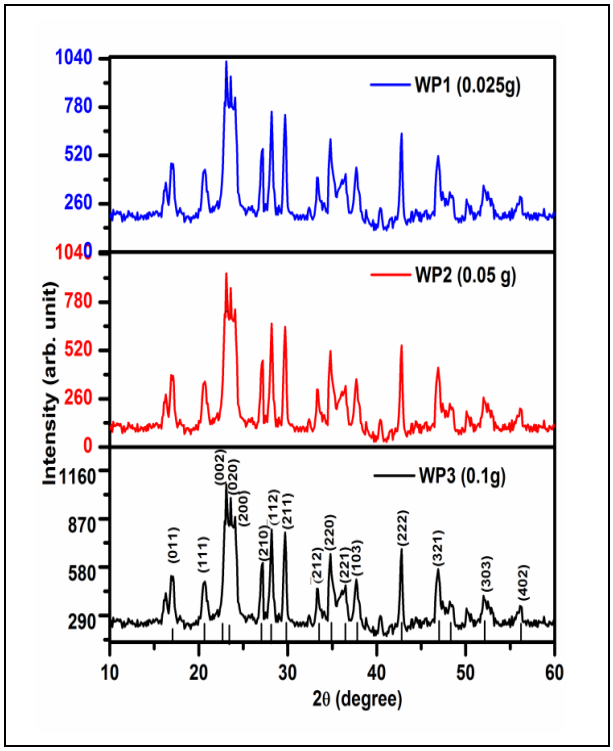

Fig. 1: X-ray diffraction pattern of WO_3 with different PVP content

Dielectric loss i.e. tan δ represents the dissipation of energy in the dielectric system. It can be explained on the basis of the relationship between dielectric behavior and conducting mechanism of the synthesized $_{sample}$. The graph shows that, the value of tan δ decreases with the increase of frequency for all the samples. On the other hand, the maximum loss has been obtained for WP1 sample which decreases after increasing PVP content (WP2, WP3) and is gradually decreases in the higher frequency regime. The high values of dielectric loss may be due to the space charge polarization. (El-Nahass *et al*. 2012).

The total conductivity (σ_T) of the sample can be calculated by the following relation (Jonscher 1977);

$$\sigma_T = \sigma_{dc(0)} + \sigma_{ac} \text{------(2)}$$

where σ_{dc} is DC conductivity which is independent of applied frequency and σac is AC conductivity depends on applied frequency. Fig. 4 depicted the AC electrical conductivity of all samples. Its arise due to migration of the electric charge in between W^{6+} and W^{5+} site respectively. The AC conductivity gradually increases for all the samples with the increase of frequency. It also clear $_{that}$, the maximum conductivity

is obtained for WP3 which decreases with decreasing PVP content (WP2 and WP1). The decrease of conductivity may be due to the formation of grain boundary defect barrier leading to blockage to the flow of charge carriers. As a result, the WO_3 can be used for high frequency device applications.

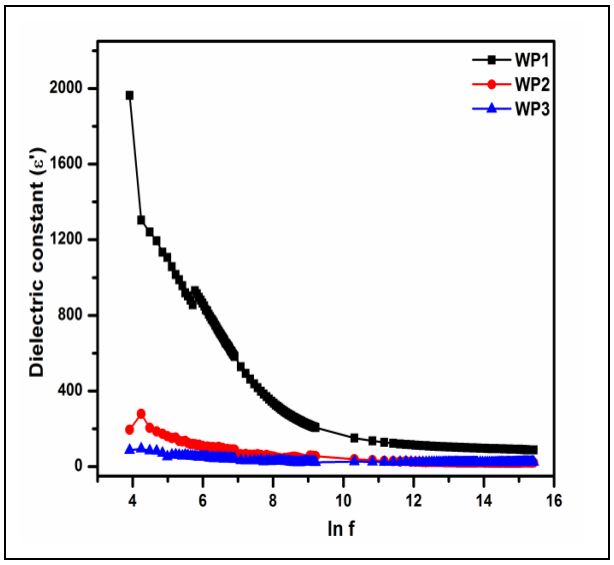

Fig. 2: The frequency dependence of dielectric constant (ε') at room temperature

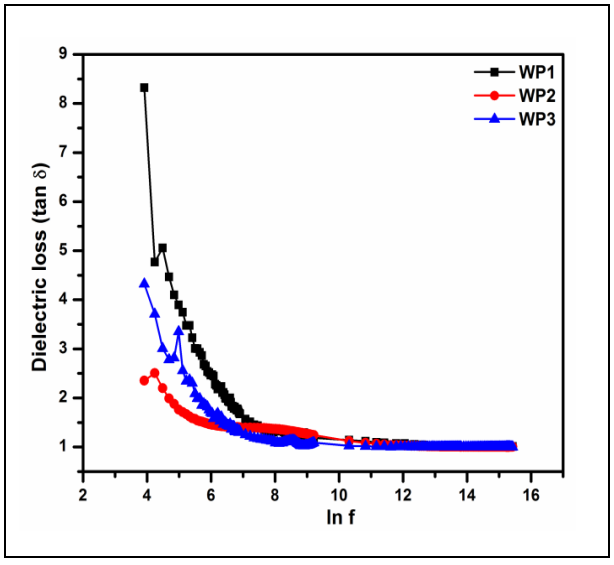

Fig. 3: The frequency dependence of dielectric loss (tan δ) at room temperature

The temperature dependence of DC electrical conductivity (σ_{dc}) can be explained by an empirical Arrhenius relation (Hutchins *et al.* 2006):

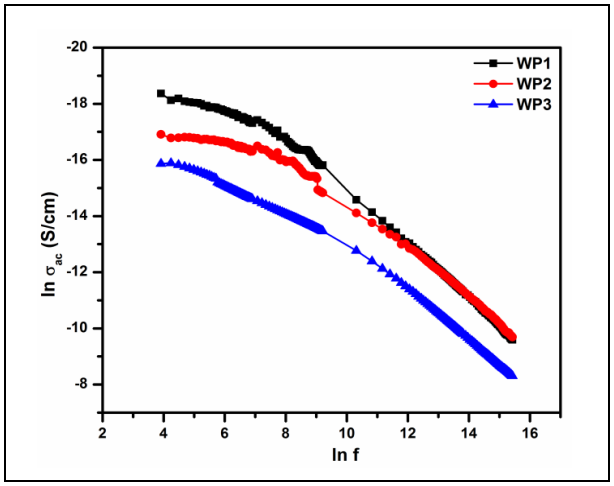

Fig. 4: The frequency dependence of AC electrical conductivity (σ_{ac}) at room temperature

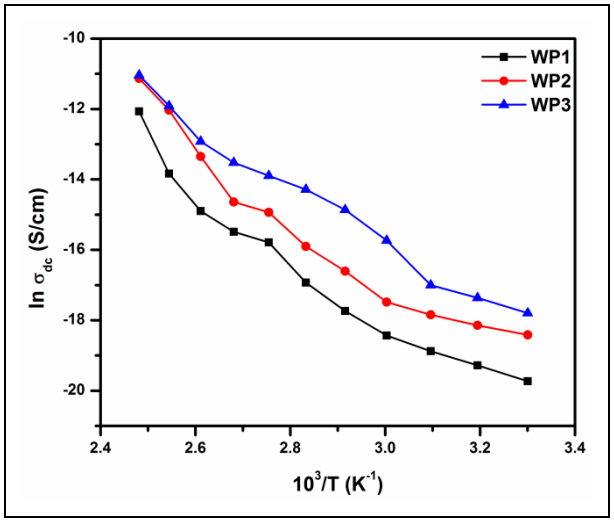

Fig. 5: Activation energy of ln σ_{dc}(S/cm) vs $10^3/T$ (K^{-1})

$$\sigma_{dc} = \sigma_0 \exp\left(\frac{-E_a}{k_b T}\right) ------(3)$$

where σ_0 is the pre-exponential factor, E_a is the activation energy and k_b is the Boltzmann constant. The conductivity (σ_{dc}) of WO_3 with different PVP samples as a function of temperature as shown in the Fig.5. It is observed that, the electrical conductivity increases with increasing temperature for the all sample showing the semiconductor nature (M. Gillet *et al.*, 2004). Fig. 5 shows the Arrhenius plot of ln σ_{dc} versus 1/T (10^3 K^{-1}). The slope taken from the graph gives the information about the activation energy in the temperature range 303-

403 K. The calculated activation energy is 0.79, 0.61 and 0.52 eV for WP1, WP2 and WP3 respectively. It is clear that, the activation energy decreases with increasing PVP content and temperature.

The calculated activation results were compared with previous report (A. Al Mohammad 2009). An increase in DC conductivity with corresponding decrease in activation energy is found to be associated with hopping of charge carrier in localized state. From the above results we can conclude that hopping mechanism is responsible for increase in the conductivity of the samples.

4. CONCLUSION

WO3 nanoparticles were successfully synthesized by low cost wet chemical method with PVP. The obtained XRD showed that the monoclinic structure of WO_3. The dielectric constant, dielectric loss and AC conductivity were investigated. DC electrical conductivity was measured for all the prepared samples conductivity in the temperature range 303-403 K. The temperature dependence of electrical conductivity is decreases with increasing PVP content. The conductivity increases with increasing the temperature showing the semiconducting nature of the samples. From the Arrhenius plot, activation energies are calculated. The observed value of electrical and dielectric constant shows that the synthesized WO_3 is a good for high frequency device applications.

FUNDING

This research received no specific grant from any funding agency in the public, commercial, or not-for-profit sectors.

CONFLICTS OF INTEREST

The authors declare that there is no conflict of interest.

REFERENCES

Al Mohammad. A,Synthesis, Separation and Electrical Properties of WO_{3-x} Nanopowders via Partial Pressure High Energy Ball-Milling, *ACTA Physica Polonica A*, 116(2), 240-244(2009).

Ansari. S.A, Nisar. A, Fatma .B, Khan. W, Naqvi .A, Investigation on structural, optical and dielectric properties of Co doped ZnO nanoparticles synthesized by gel-combustion route.*Mater. Sci. Engg*., B, 177, 428-435(2012). https://doi.org/10.1016/j.mseb.2012.01.022

Diah Susanti, Gede Pradnyana Diputra A. A., Lucky Tananta, Hariyati Purwaningsih, George Endri Kusuma, Chenhao Wang, Shaoju Shih and Yingsheng Huang, WO_3 nanomaterials synthesized via a sol-gel method and calcination for use as a CO gas sensor, *Frontiers of Chemical Science and Engineering*, 8(2), 179–187(2014). https://doi.org/10.1007/s11705-014-1431-0

Dirany. N, Arab. M., Madigou.V., Leroux. Ch and Gavarri . J. R., A facile one step route to synthesize WO_3 nanoplatelets for CO oxidation and photodegradation of RhB: microstructural, optical and electrical studies, *RSC Adv.*, 6, 69615-69626(2016). https://doi.org/10.1039/C6RA13500E

El-Nahass. M.M, Ali. H.A.M, Saadeldin. M, Zaghllol. M, AC conductivity and dielectric properties of bulk tungsten trioxide (WO_3), *Physica B*, 407, 4453–4457(2012). https://doi.org/10.1016/j.physb.2012.07.043

Gillet .M, Aguir.K, Lemire .C, Gillet .E and Schierbaum. K., The structure and electrical conductivity of vacuum-annealed WO_3 thin films, *Thin Solid Films*, 467(1–2), 239–246 (2004). https://doi.org/10.1016/j.tsf.2004.04.018

Huirache-Acuna. R, Paraguay-Delgado.F, Albiter. M.A, Lara-Romero .J and Martínez-Sánchez .R, Synthesis and characterization of WO_3 nanostructures prepared by an aged-hydrothermal method, *Mater. Charact.* 60 (9), 932–937 (2009). https://doi.org/10.1016/J.MATCHAR.2009.03.006

Hutchins. M. G, Abu-Alkhair. O, MMEl-Nahass and Abdel-Hady. K Electrical conduction mechanisms in thermally evaporated tungsten trioxide *(WO_3)* thin films, *J. Phys.: Condens. Matter*, 18, 9987–9997(2006). https://doi.org/10.1088/0953-8984/18/44/001

Jianhua Hao,. Studenikin. S. A, and Michael Cocivera, Transient photoconductivity properties of tungsten oxide thin films prepared by spray pyrolysis, *J. Appl. Phys*., 90 (10) 5064-5069(2001). https://doi.org/10.1063/1.1412567

Joni Huotari, Jyrki Lappalainen, Jarkko Puustinen, Tobias Baur, Christine Alépée, Tomi Haapalainen, Samuli Komulainen, Juho Pylvänäinen and Anita Lloyd Spetz, Pulsed Laser Deposition of Metal Oxide Nanoparticles, Agglomerates, and Nanotrees for Chemical Sensors *procedia engineering* , 120, 1158-1161(2015). https://doi.org/10.1016/j.proeng.2015.08.745

Jonscher . A. K. The 'universal' dielectric response *Nature* 267, 673-679 (1977) https://doi.org/10.1038/267673a0

Pechini Maggio P. Barium, titanium citrate, barium titanate and process for producing same. Unite States Patent. No.3231328, (1966).

Powder Diffraction File, JCPDS-ICDD," 12Campus Boulevard, Newtown Square, Pa, USA, (2001).

Sandra Hilaire, Martin J. Süess, Niklaus Kränzlin, Krzysztof Bieńkowski, Renata Solarska, Jan Augustyński and Markus Niederberger, *J. Mater. Chem. A*, **,2,** 20530-20537(2014). https://doi.org/10.1039/C4TA04793A

Shaltout , Yi Tang , Braunstein. R , E.E. Shaisha. R., FTIR spectra and some optical properties of tungstate-tellurite glasses, *J. Phy. Chem. Solids*, 57(9), 1223-1230(1996). https://doi.org/10.1016/0022-3697(95)00309-6

Yoji Yamada, Kenji Tabata and Tatsuaki Yashima, The character of WO_3 film prepared with RF sputtering, *Sol. Energ. Mat. Sol. Cells* 91(1), 29-37(2007). https://doi.org/10.1016/j.solmat.2005.11.014